

# Blind Deconvolution Using Generalized Cross-Validation Approach to Regularization Parameter Estimation

Haiyong Liao and Michael K. Ng

**Abstract**—In this paper, we propose and present an algorithm for total variation (TV)-based blind deconvolution. Both the unknown image and blur can be estimated within an alternating minimization framework. With the generalized cross-validation (GCV) method, the regularization parameters associated with the unknown image and blur can be updated in alternating minimization steps. Experimental results confirm that the performance of the proposed algorithm is better than variational Bayesian blind deconvolution algorithms with Student’s-t priors or a total variation prior.

**Index Terms**—Alternating minimization, blind deconvolution, generalized cross validation (GCV), regularization parameters, total variation (TV).

## I. INTRODUCTION

IMAGE restoration problems have always been important image processing tasks with many real-world applications. The blurring of images often occurs from the motion of objects, unfocused cameras, and calibration errors with imaging devices. Mathematically, the forward model of the blurring process is stated as

$$g(x, y) = h(x, y) \otimes f(x, y) + n(x, y) \quad (1)$$

in the continuous setting. Here,  $g(x, y)$  is the degraded image,  $f(x, y)$  is the original image,  $h(x, y)$  is the point spread function (PSF) representing the characteristic of the imaging system,  $n(x, y)$  is the additive noise, and  $\otimes$  is the convolution operator. For clarity, the spatial coordinates would be omitted in the following. While nonblind deconvolution theoretically provides the best results, the required PSF  $h$  may not be easily and accurately obtained. The blind deconvolution task amounts to recovering  $f$  and  $h$  given only the degraded image  $g$ , for example, in remote sensing and astronomical imaging and many other blind deconvolution applications [25].

Manuscript received December 16, 2009; revised June 14, 2010; accepted August 27, 2010. Date of publication September 07, 2010; date of current version February 18, 2011. This work was supported in part by grants from the Hong Kong Research Grant Council and Hong Kong Baptist University Faculty Research Grant. The associate editor coordinating the review of this manuscript and approving it for publication was Dr. Yongyi Yang.

The authors are with the Centre for Mathematical Imaging and Vision and Department of Mathematics, Hong Kong Baptist University, Kowloon Tong, Hong Kong (e-mail: 06459358@hkbu.edu.hk; mng@math.hkbu.edu.hk).

Color versions of one or more of the figures in this paper are available online at <http://ieeexplore.ieee.org>.

Digital Object Identifier 10.1109/TIP.2010.2073474

There are many methods for simultaneous recovery of the deblurred image  $f$  and the PSF  $h$  in (1), which include inverse filtering methods [1]–[3], statistical estimation methods [4]–[11], spectral and cepstral zero estimation methods [12]–[14], learning-based methods [15], [16], Tikhonov regularization [17], total variation (TV) regularization [18]–[21] methods, and projection-based method [23]. The reader is referred to a survey and book on blind image deconvolution [24], [25].

As the blind image deconvolution is an ill-posed problem, You and Kaveh [17] proposed regularizing  $f$  and  $h$  by considering the following joint minimization problem:

$$\min_{f, h} \|f \otimes h - g\|_2^2 + \alpha_1 \|Df\|_2^2 + \alpha_2 \|Dh\|_2^2 \quad (2)$$

where  $D$  is the first-order differencing matrix,  $\alpha_1$  and  $\alpha_2$  are the two positive regularization parameters which measure the trade off between a good fit and the regularity of the solutions  $f$  and  $h$ . One of the useful regularization approaches is the TV regularization method [26], which can effectively recover edges of an image or a blur. In [20], You and Kaveh employed the anisotropic diffusion method for recovering  $f$  and  $h$ . Chan and Wong [18] further studied the following blind deconvolution problem:

$$\min_{f, h} \|f \otimes h - g\|_2^2 + \alpha_1 TV(f) + \alpha_2 TV(h). \quad (3)$$

The definition of discrete TV norm will be given in Section II. Chan and Wong devised an alternating minimization scheme for solving (3), but the regularization parameters  $\alpha_1$  and  $\alpha_2$  must be chosen correctly so that both  $f$  and  $h$  can be recovered properly. Similarly, in [21], Huang and Ng followed the same approach, but they used Lipschitz regularization instead of the TV regularization for image estimation. In their test, they showed that they had a better result than those with TV regularization for image restoration. However, in all of these approaches, the regularization parameters must be determined properly so that the algorithm can provide good recovered images and blurs. In [18] and [21], methods are not given for searching suitable regularization parameters.

On the other hand, Bayesian methods are commonly used methods in blind deconvolution. Such methods incorporate prior

models on the image, blur and their associated regularization parameters. It is known that the exact posterior distribution is very hard to compute. Variational Bayesian methods in blind deconvolution are employed to approximate the posterior via minimizing the Kullback–Leibler (KL) divergence related to the posterior distribution. In [7], Molina *et al.* proposed the use of simultaneous autoregressive (SAR) as prior distributions for both the image and blur, gamma distributions for the unknown parameters (hyperparameters) of the priors, and the image formulation noise. They applied variational methods to approximate the posterior probability of the unknown image, blur, and hyperparameters and proposed two different approximations of the posterior distribution. In [19], Babacan *et al.* proposed using variational methods for the blind deconvolution problem by incorporating a TV function as the image prior and a SAR model as the blur prior. This is the first work on the simultaneous estimation of the model parameters, image, and blur based on TV function as the image prior. Their experimental results have shown that the proposed method provides high-resolution performance than non-TV-based methods without any assumptions about the unknown hyperparameters. In [8], Tzikas *et al.* employed a sparse kernel-based model for the point spread function and used priors that are based on the Student's-t probability density function. Their numerical experiments have shown that the performance of their method is better than that using Gaussian priors and TV-based methods. The advantage of these methods is that the associated regularization parameters can be obtained via variational Bayesian learning.

In this paper, we formulate the blind deconvolution as follows:

$$\min_{f,h} J(f,h) \equiv \min_{f,h} \|f \otimes h - g\|_2^2 + \alpha_1 TV(f) + \alpha_2 \|Lh\|_2^2 \quad (4)$$

where  $L$  is the discrete Laplacian (second-order differencing) matrix. This formulation is different from (2) and (3). We regularize the image by the total variational norm and the blur by the squares of the Euclidean norm of the second-order difference among the pixels (this is the analog to the  $H^2$  norm in the function space). The regularization term  $\|Lh\|_2^2$  is effective in estimating smooth point spread functions like Gaussian blurs; see [19]. For piecewise smooth point spread functions like out-of-focus blurs, we find in our numerical examples in Section III that the performance of using  $\|Lh\|_2^2$  is much better than that of using TV norm. We remark that the formulation in (4) is equivalent to using a TV function as the image prior and a SAR model as the blur prior under the Bayesian setting [19]. However, Babacan *et al.* [19] used the variational Bayesian method to estimate the regularization parameters. In [22], we have successfully used the generalized cross validation (GCV) method for image restoration (nonblind deconvolution). In [22], the GCV method is only applied to estimate the regularization parameter associated to total variation function.

In this work, the main contribution is to develop an algorithm for TV-based blind deconvolution and make use of the GCV method to estimate both the regularization parameters  $\alpha_1$

and  $\alpha_2$  in (4) for the image and the blur. We design the GCV method to deal with the estimation of the two regularization parameters which are crucial in blind deconvolution. In the algorithm, the two regularization parameters, the unknown image and the unknown blur can be estimated within alternating minimization framework. However, in the variational Bayesian approaches, approximations are required in their computational steps. Therefore, their resulting solutions may not be exact. Here the proposed approach solves the blind deconvolution problem by using alternating minimization and GCV methods for estimation of regularization parameters without approximation. Numerical examples are presented to illustrate the performance of the proposed method is better than the other algorithms like variational Bayesian blind deconvolution algorithms with Student's-t priors or a total variation prior.

The outline of this paper is as follows. In Section II, we present our algorithm. In Section III, we present experimental results. Conclusions are drawn in Section IV.

## II. GCV-BASED BLIND DECONVOLUTION ALGORITHM

### A. Discrete Total Variation

It is well known that the TV model proposed by Rudin *et al.* [26] is a very successful method for image restoration because of its ability to preserve edges in the image due to the piecewise constant regularization property of the TV norm. The discrete version of the TV regularization term is given as follows. The discrete gradient operator  $\nabla : \mathbb{R}^{n^2} \rightarrow \mathbb{R}^{n^2}$  is defined by

$$(\nabla f)_{j,k} = ((\nabla f)_{j,k}^x, (\nabla f)_{j,k}^y)$$

with

$$(\nabla f)_{j,k}^x = \begin{cases} f_{j+1,k} - f_{j,k}, & \text{if } j < n \\ 0, & \text{if } j = n \end{cases}$$

$$(\nabla f)_{j,k}^y = \begin{cases} f_{j,k+1} - f_{j,k}, & \text{if } k < n \\ 0, & \text{if } k = n \end{cases}$$

for  $j, k = 1, \dots, n$ . Here,  $f_{j,k}$  refers to the  $(jn + k)$ th entry of the vector  $f$  (it is the  $(j, k)$ th pixel location of an  $n \times n$  image). The discrete total variation of  $f$  is defined by

$$TV(f) := \sum_{1 \leq j,k \leq n} \sqrt{|(\nabla f)_{j,k}^x|^2 + |(\nabla f)_{j,k}^y|^2}.$$

### B. Alternating Minimization Scheme

An alternating minimization scheme is employed to recover the image and simultaneously identify the point spread function. We note that, for a given  $h$ ,  $J(., h)$  in (4) is a convex function with respect to  $f$ . Similarly, for a given  $f$ ,  $J(f, .)$  in (4) is a convex function with respect to  $h$ . Therefore, with an initial guess of image and PSF  $(f_0, h_0)$  for  $(f, h)$ , we can minimize (4) by first solving  $f_1 = \arg \min_f J(f, h_0)$  and then solving  $h_1 = \arg \min_h J(f_1, h)$ . This alternating minimization algorithm decreases the function value  $J(f_n, h_n)$  as  $n$  increases. Such an alternating minimization framework has been considered and studied by [17]–[22]. We summarize the iterative procedure in Algorithm 1.

---

**Algorithm 1** Alternating Minimization Algorithm for Blind Deconvolution
 

---

1: Input: an initial image  $f_0$ , an initial PSF  $h_0$  and an observed image  $g$

2: Let  $n = 1$  and  $\epsilon_f$  and  $\epsilon_h$  be a threshold for the stopping criterion

3: Solve for  $f_n$ :

$$\begin{aligned} f_n &= \arg \min_f J(f, h_{n-1}) \\ &= \arg \min_f \|h_{n-1} \otimes f - g\|_2^2 + \alpha_1 TV(f) \end{aligned} \quad (5)$$

4: Solve for  $h_n$ :

$$\begin{aligned} h_n &= \arg \min_h J(f_n, h) \\ &= \arg \min_h \|h \otimes f_n - g\|_2^2 + \alpha_2 \|Lh\|_2^2 \end{aligned} \quad (6)$$

5: **if**  $|f_n - f_{n-1}|/|f_{n-1}| \leq \epsilon_f$  or  $|h_n - h_{n-1}|/|h_{n-1}| \leq \epsilon_h$  **then**

6: Go to Step 10

7: **else**

8:  $n = n + 1$

9: Go to Step 3

10: **end if**

11: Output: the restored image  $f_n$  and the restored PSF  $h_n$ .

Without using *a priori* information, we set  $f_0$  to be the observed image and  $h_0$  to be the delta function (that is, its function value is one at the origin and zero elsewhere) in our experimental results. The minimization problem (4) may not have a unique solution. In order to obtain a physically meaningful solution, we need to impose natural and physical conditions on  $f$  and  $h$ . Similar to the conditions given in [18], we impose the following conditions:

$$\sum_{i,j} [h]_{i,j} = 1 \quad [h]_{i,j} = [h]_{j,i}, \quad h \geq 0 \text{ and } f \geq 0.$$

That is to say,  $f$  and  $h$  should be nonnegative,  $h$  is symmetric, and summation of entries of  $h$  is 1. In the above algorithm, we need to solve for  $f$  and  $h$  in steps 3 and 4, respectively. For these two steps, the most importance is that we need to select suitable regularization parameters  $\alpha_1$  and  $\alpha_2$  in steps 3 and 4 so that well-restored image and PSF can be obtained by the algorithm. We discuss these estimation issues in the next sections.

### C. Restoration of Images and PSFs

A number of numerical methods have been proposed for solving (5), for instance, artificial time marching, primal-dual method, and lagged-diffusivity, Newton's method; see for instance [27] for references therein. Recently, Huang *et al.* [28] proposed and developed a fast total variation minimization

method for TV image-restoration model. In their paper, an auxiliary variable and an additional quadratic term is added to the objective function (5). In the alternative minimization framework, minimizing the new objective function can be interpreted as a two-stage process, i.e., denoising and deblurring. Experimental results in [28] have shown that the quality of restored images by their method are competitive with those restored by the existing TV restoration methods. This approach has also been successfully used for  $l_1$  data fitting term [29]. Recently, Wang *et al.* [30], [31] also proposed and developed the alternating minimization algorithm for deblurring and denoising jointly by solving a TV regularization problem. Their algorithm is derived from the well-known variable-splitting and penalty techniques in optimization. The idea is to use auxiliary variables to replace the gradients in nondifferentiable TV term and make the auxiliary variables close to the gradients by the quadratic penalty approach. Extensive numerical results show that their algorithm performs favorably in comparison with several state-of-the-art algorithms.

Here, we adapt the idea by adding an auxiliary variable  $\bar{f}$  to the problem and an additional term which measures the difference between  $f$  and  $\bar{f}$  in terms of the squares of the Euclidean norm, i.e.,

$$\min_{f, \bar{f}} \left\{ \frac{1}{\alpha_1} \|h \otimes f - g\|_2^2 + \frac{\beta}{2} \|f - \bar{f}\|_2^2 + TV(\bar{f}) \right\}. \quad (7)$$

It is noted that (7) is close to (5) when  $\beta$  is sufficiently large. Here, (7) is solved for  $f$  given  $\bar{f}$ , and (7) is solved for  $\bar{f}$  given  $f$ . The iterative algorithm is summarized in Algorithm 2.

---

**Algorithm 2** Image Estimation Algorithm
 

---

1: Input: the current image  $f_{n-1}$ , the current PSF  $h_{n-1}$ , and an observed image  $g$

2: Initialize  $\beta$  and  $\theta$  (the multiplier), and set  $\epsilon$  to be the stopping criterion and  $\bar{f} = f_{n-1}$  (the current estimate of  $f$ )

3: Solve  $\min_f \|h_{n-1} \otimes f - g\|_2^2 + \alpha_1 \beta / 2 \|f - \bar{f}\|_2^2$

4: Solve  $\min_{\bar{f}} \beta / 2 \|\bar{f} - f\|_2^2 + TV(\bar{f})$

5:  $\beta = \theta \cdot \beta$  (the increase of  $\beta$ )

6: **if** the relative error of the successive iterate  $\bar{f}$  is less than  $\epsilon$  **then**

7: Go to Step 11

8: **else**

9: Go to Step 3

10: **end if**

11: Output:  $f_n = \bar{f}$ .

In Algorithm 2, Steps 3 and 4 can be considered as image deblurring and denoising, respectively. In Step 3, After discretization, the problem is equivalent to solving a linear system  $(H^* H + \mu I) f = H^* g + \mu \bar{f}$ , where  $H$  is the blurring matrix derived from the PSF  $h$ ,  $*$  denotes the conjugate transpose of a matrix, and  $\mu = \alpha_1 \beta / 2$ . Such a linear system can be solved by

fast transform-based methods and preconditioning techniques for Toeplitz-like matrices; see [32]. For instance, when  $H$  is diagonalized by the discrete Fourier transform matrix  $F$ , i.e.,  $H = F^* \Lambda F$  and  $\Lambda$  is a diagonal matrix containing the eigenvalues of  $H$ . We note that the closed form solution of the linear system is

$$f = F^* \left[ (\Lambda^* \Lambda + \mu I)^{-1} (\Lambda^* \hat{g} + \mu \hat{f}) \right] \quad (8)$$

where  $\hat{f} = Ff$ ,  $\hat{f} = F\bar{f}$ , and  $\hat{g} = Fg$ . For the denoising problem in Step 4, the solution can be computed by many total variation denoising methods like Chambolle's projection algorithm [33] or semismooth Newton's method [34].

On the other hand, for the estimation of PSF in (6), it can be solved efficiently in the frequency domain. The closed-form solution of (6) is given by

$$h = F^* \left[ (\Gamma^* \Gamma + \alpha_2 \Omega^* \Omega)^{-1} (\Gamma^* \hat{g}) \right] \quad (9)$$

where  $\Gamma = \text{diag}(\hat{f})$  (it is a diagonal matrix with diagonal entries being equal to  $\hat{f}$ ), and  $L$  can be diagonalized by the discrete Fourier matrix  $F$ , i.e.,  $L = F^* \Omega F$  and  $\Omega$  is a diagonal matrix containing the eigenvalues of  $L$ .

#### D. Estimation of Regularization Parameters

GCV [35] is a technique that estimates a parameter directly without any knowledge on noise. The basic idea is to take  $k$ th observation out of all observed data and then to use the remaining observations to predict the  $k$ th observation. If a parameter is a good choice, the overall prediction error would be minimized. Therefore, the best parameter can be determined by finding the minimum value of the overall prediction error, i.e., the GCV function. In [9], Reeves and Mersereau modeled the image as a 2-D autoregressive process, and the degraded image as a 2-D moving average process. They used the GCV method to estimate the parameters of these autoregressive and moving average processes. When there are several parameters to be estimated, the associated GCV function are quite complicated. Reeves and Mersereau proposed to solve this problem by estimating a parameter one by one and fixing the other parameters in the process. It is obvious that this procedure can be quite time-consuming when the number of parameters is huge.

In this paper, we use a total variation function as the image prior and a SAR model as the blur prior; see [19]. We employ the GCV method to find the regularization parameters  $\mu$  (or  $\alpha_1/\beta/2$ ) in Step 3 of Algorithm 2 and  $\alpha_2$  in Step 4 of Algorithm 1. In our consideration, we can estimate these two parameters separately and restore images and PSFs after these parameters are obtained in Algorithms 1 and 2.

For the estimation of  $\alpha_2$ , we first rewrite (6) in the frequency domain as follows:

$$\min_{\hat{h}} \|\Gamma \hat{h} - \hat{g}\|_2^2 + \alpha_2 \|\Omega \hat{h}\|_2^2$$

where  $\hat{h} = Fh$ . Here we assume  $\Omega$  is invertible. Then, the above optimization problem is equivalent to

$$\min_{\hat{h}'} \|\Gamma \Omega^{-1} \hat{h}' - \hat{g}\|_2^2 + \alpha_2 \|\hat{h}'\|_2^2. \quad (10)$$

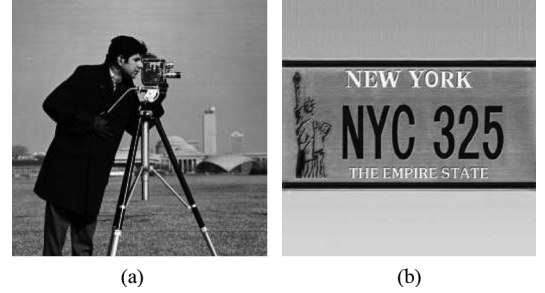


Fig. 1. Original images. (a) Cameraman. (b) CarNo.

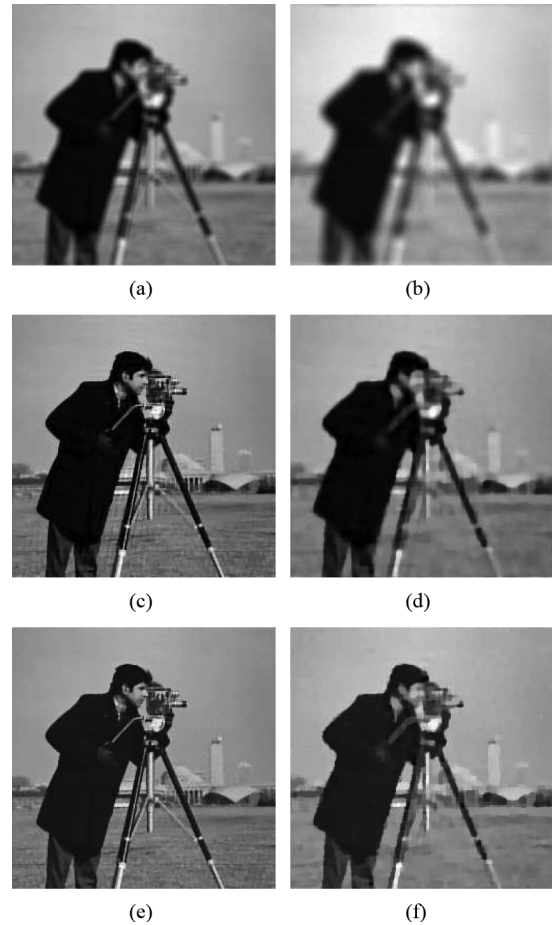


Fig. 2. Cameraman. Observed images: (a) Gaussian PSF of ( $hsize = 7$ ,  $\sigma^2 = 25$ ), BSNR = 40 dB. (b) Gaussian PSF of ( $hsize = 14$ ,  $\sigma^2 = 25$ ), BSNR = 30 dB. Restored images: (c), (d) by the proposed GCV-BD algorithm and (e), (f) by the nonblind deconvolution method in [28].

Note that both  $\Gamma$  and  $\Omega$  are diagonal matrices. By using the results in [36] and [37], it can be shown that the GCV function of  $\alpha_2$  for (10) is given by

$$GCV_h(\alpha_2) = n^2 \frac{\sum_{i=1}^{n^2} \left( \frac{|[\Omega]_{ii}|^2 |[\hat{g}]_i|}{|[\Gamma]_{ii}|^2 + \alpha_2 |[\Omega]_{ii}|^2} \right)^2}{\left( \sum_{i=1}^{n^2} \frac{|[\Omega]_{ii}|^2}{|[\Gamma]_{ii}|^2 + \alpha_2 |[\Omega]_{ii}|^2} \right)^2}. \quad (11)$$

If  $\Omega$  is not invertible, we can replace  $\Omega$  by  $\Omega + \tau I$ , where  $\tau$  is a positive number. In this case, the GCV function can be derived

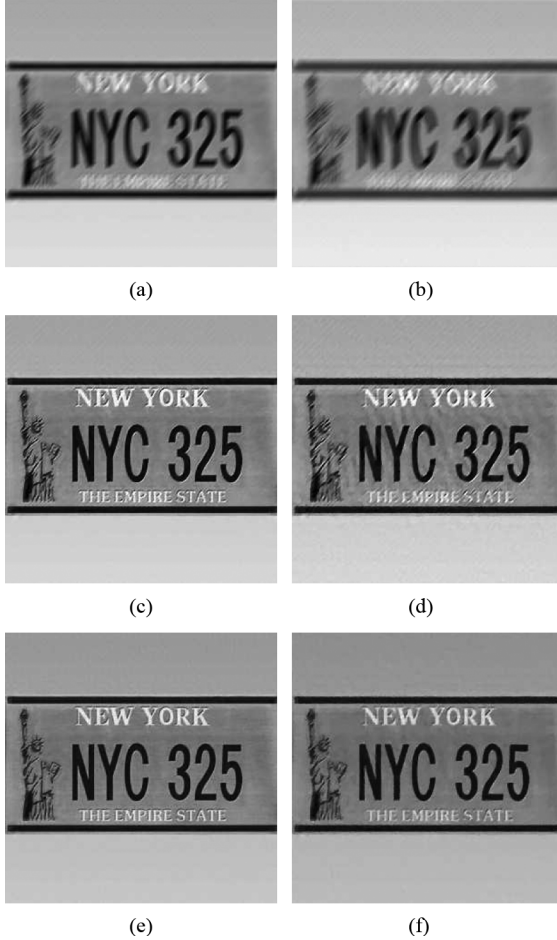


Fig. 3. CarNo. Observed images. (a) Motion PSF of length 9, BSNR = 40 dB. (b) Motion PSF of length 15, BSNR = 30 dB. Restored images: (c), (d) by the proposed GCV-BD algorithm and (e), (f) by the nonblind deconvolution method in [28].

TABLE I  
COMPARISON IN TERMS OF SNR ON THE PROPOSED GCV-BD ALGORITHM  
AND NONBLIND DECONVOLUTION ALGORITHM [28]

Image	PSF/BSNR	GCV-BD	Non-blind [28]
Cameraman	Gaussian(7,5)/40	16.71	18.13
Cameraman	Gaussian(14,5)/30	10.65	12.10
CarNo	Motion(9)/40	18.33	22.03
CarNo	Motion(15)/30	14.04	16.75

similar to (11) except that  $[\Omega]_{ii}$  is replaced by  $[\Omega]_{ii} + \tau$ . Now, we obtain the limiting GCV function of  $\alpha_2$  by considering that  $\tau$  tends to zero. The resulting GCV function is just the same as (11). The optimal regularization parameter  $\alpha_2$  can be chosen to be the one that minimizes  $GCV_h(\alpha_2)$ . Since the GCV function is a nonlinear function, the minimizer usually cannot be determined analytically. Numerical techniques can be used to determine the optimal  $\alpha_2$  for the minimization of  $GCV_h(\alpha_2)$ ; see, for instance, [38]. In our implementation, we use golden section search and parabolic interpolation to find the minimizer; see [39] and [40].

Next, we consider the regularization parameter  $\mu$  for the restoration of images. In Step 3 of Algorithm 2, we solve a

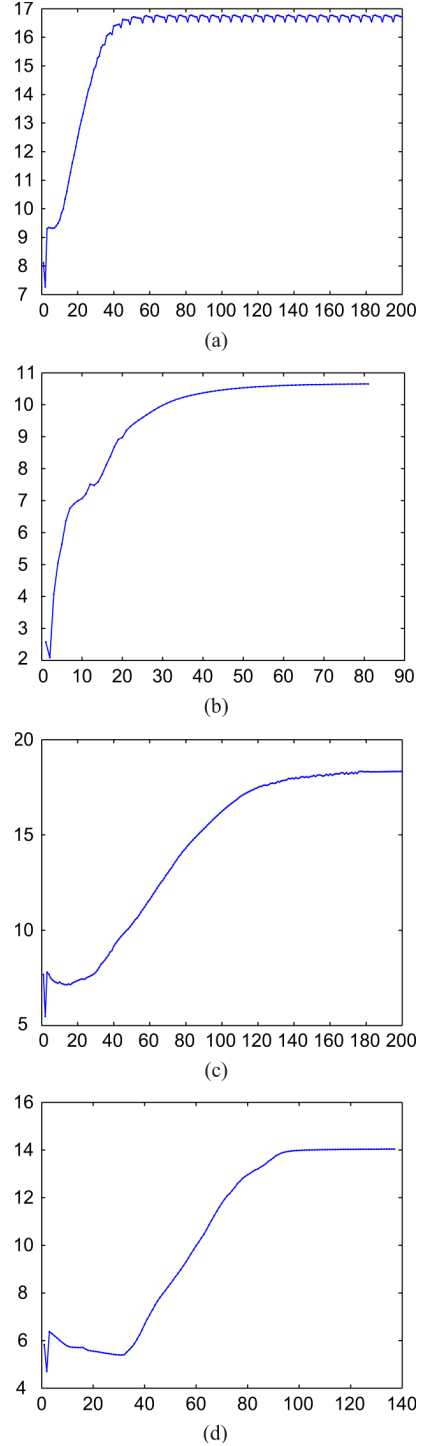


Fig. 4. SNRs with respect to number of iterations. (a) Cameraman, Gaussian(7,5), BSNR = 40. (b) Cameraman, Gaussian(14,5), BSNR = 30. (c) CarNo, Motion(9), BSNR = 40 dB. (d) CarNo, Motion(15), BSNR = 30 dB.

linear least squares problem with Tikhonov regularization. In the transform domain, it is equivalent to

$$\min_{\hat{f}} \|\Lambda \hat{f} - \hat{g}\|_2^2 + \mu \|\hat{f} - \tilde{\hat{f}}\|_2^2. \quad (12)$$

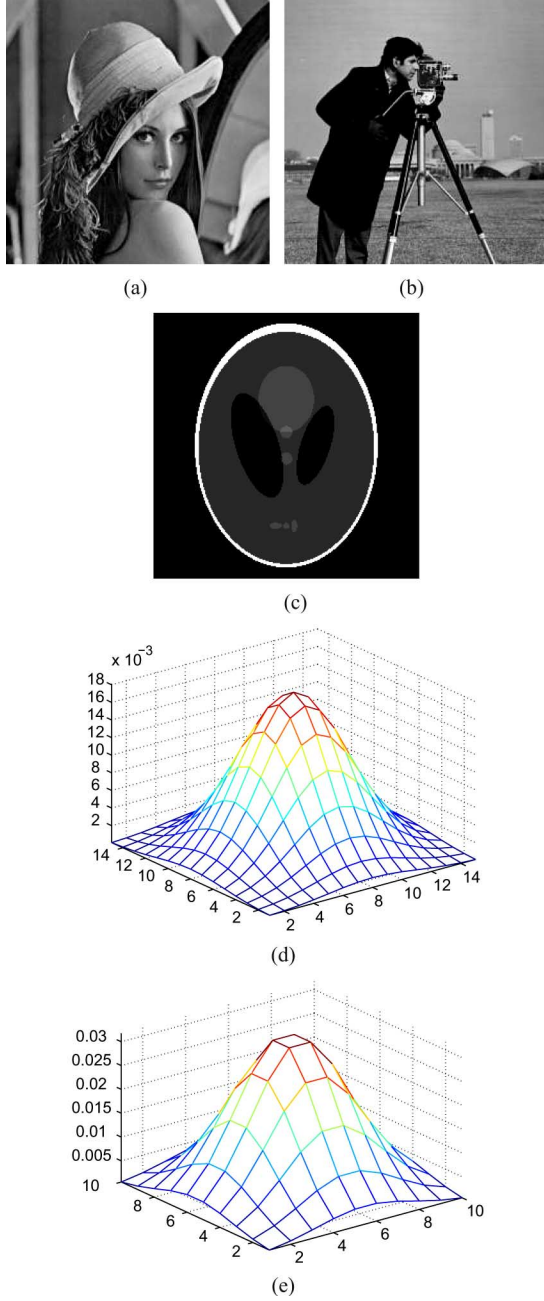


Fig. 5. Original images and PSFs. (a) Lena. (b) Cameraman. (c) Shepp-logan. (d) Gaussian PSF with variance 9. (e) Gaussian PSF with variance 5.

Similar to the GCV parameter estimation of  $\alpha_2$ , we can construct the GCV function of  $\mu$  for (12), and it is given by

$$GCV_f(\mu) = n^2 \frac{\sum_{i=1}^{n^2} \left( \frac{|\hat{g} - \Lambda \hat{f}|}{\|\Lambda\|_{ii}^2 + \mu} \right)^2}{\left( \sum_{i=1}^{n^2} \frac{1}{\|\Lambda\|_{ii}^2 + \mu} \right)^2}. \quad (13)$$

Similarly, numerical techniques can be applied to find the optimal  $\mu$  for the minimization of  $GCV_f(\mu)$ . We note that it is not necessary to compute the trace of the influence matrix in

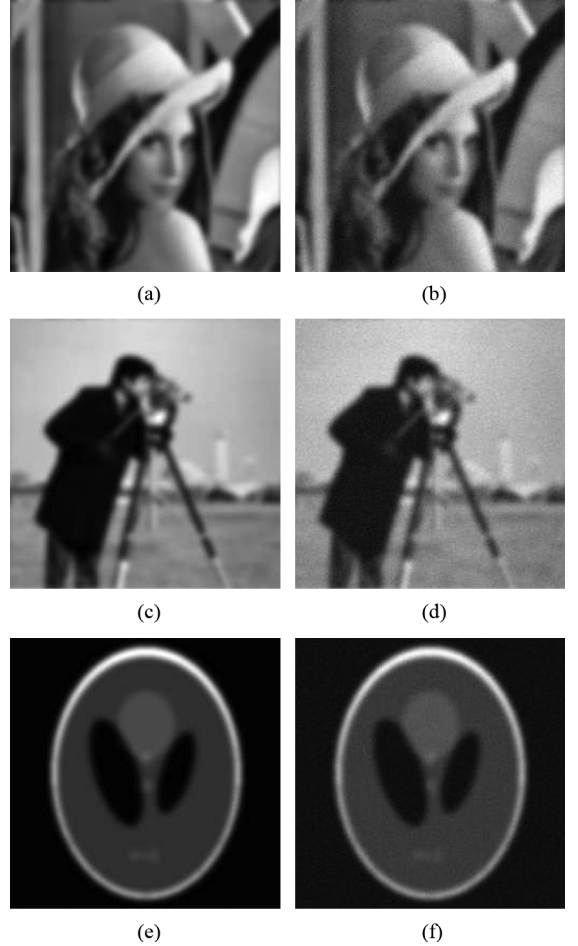


Fig. 6. Observed images. Gaussian PSF with variance 9, BSNR = 40 dB (left) and 20 dB (right).

the GCV functions. The search of  $\mu$  and  $\alpha_2$  in (13) and (11) involves scalar arithmetic operations, and  $[\Lambda]_{ii}$ ,  $[\Omega]_{ii}$ , and  $[\Gamma]_{ii}$  are calculated by using fast Fourier transforms, and therefore these computational tasks are efficient. In Section III, we will show the performance of the proposed GCV-based blind deconvolution algorithm.

### III. EXPERIMENTAL RESULTS

Here, we show the results obtained by the proposed GCV-based blind deconvolution (GCV-BD) algorithm. We compare the proposed algorithm with the nonblind deconvolution method in [28] where the point spread function is known. In other words, Step 4 of Algorithm 1 and the corresponding stopping criterion are removed. We also compare the proposed method with the other blind deconvolution algorithms in the literature. They are the TV blind deconvolution algorithm in [18], the variational Bayesian blind deconvolution algorithms: TV1 and TV2 [19] and StStSt [8]. The TV blind deconvolution algorithm uses total variation function as the image and the point spread function priors. Both TV1 and TV2 used the total variation function as the image prior and a simultaneous autoregressive (SAR) model as the PSF prior. It is similar to the proposed blind deconvolution



(a)

(b)

(c)

(d)

(e)

(f)

Fig. 7. Restored images. Gaussian PSF with variance 9, BSNR = 40 dB (left) and 20 dB (right).

setting. However, TV1 and TV2 employed variational Bayesian techniques to determine the parameters in the blind deconvolution problem. StStSt used a sparse kernel-based model for the point spread function and priors that are based on the Student's-t probability density function.

In the experiments, we test the proposed algorithm on several images with different kinds of PSFs and noise levels. We use blurred signal-to-noise ratio (BSNR) to measure the noise contained in observed image, and signal-to-noise ratio (SNR) and improvement in signal-to-noise ratio (ISNR) to measure the quality of restored images. They are defined as follows:

$$\begin{aligned} \text{SNR} &= 20 \log_{10} \left( \frac{\|f - \text{mean}(f)\|_2}{\|u - f\|_2} \right) \\ \text{BSNR} &= 20 \log_{10} \left( \frac{\|g\|_2}{\|n\|_2} \right) \\ \text{ISNR} &= 20 \log_{10} \left( \frac{\|f - g\|_2}{\|f - u\|_2} \right) \end{aligned}$$

where  $f$ ,  $g$ ,  $u$ , and  $n$  are the original image, observed image, recovered image, and the noise vector, respectively, and  $\text{mean}(f)$  denotes the mean of  $f$ . In all the experiments, we use an observed image as an initial image and an  $\delta$  function as an initial



(a)

(b)

(c)

(d)

(e)

(f)

Fig. 8. Observed images. Gaussian PSF with variance 5, BSNR = 40 dB (left) and 20 dB (right).

point spread function. In Algorithm 1, the constraints on image and PSF are imposed once image and PSF are obtained in each iteration. More specifically, the negative entries of the iterate image and PSF are set to zero, and the PSF is divided by the sum of all entries so that its sum becomes one. As the maximum pixel value of the original image is set to be 1, we also set the maximum pixel value of the restored image to be 1 in each iteration. For the stopping criteria,  $\epsilon_f$  and  $\epsilon_h$  are set to be  $1 \times 10^{-4}$  in Algorithm 1 and  $\epsilon$  is set to be  $1 \times 10^{-4}$  in Algorithm 2. Also the initial value of  $\beta$  and the multiplier  $\theta$  are set to be 10 and 1.2, respectively, for all of the tests. The proposed algorithm is written in MATLAB.

#### A. Comparison With the Nonblind Deconvolution Method

Two images are used to test the proposed algorithm. The first one is of size  $256 \times 256$ , and the other is of size  $301 \times 301$ . These images are shown in Fig. 1. The "Cameraman" image is blurred by Gaussian PSFs with variance 25 of sizes 7 and 14, respectively. The "CarNo" image is blurred by motion PSFs of lengths 9 and 15 pixels, respectively. Then Gaussian noise is added to each blurred image. Their resulting blurred and noisy images are shown in Figs. 2, 3(a), and 3(b). We display the restored images by the proposed GCV-BD algorithm in Figs. 2,

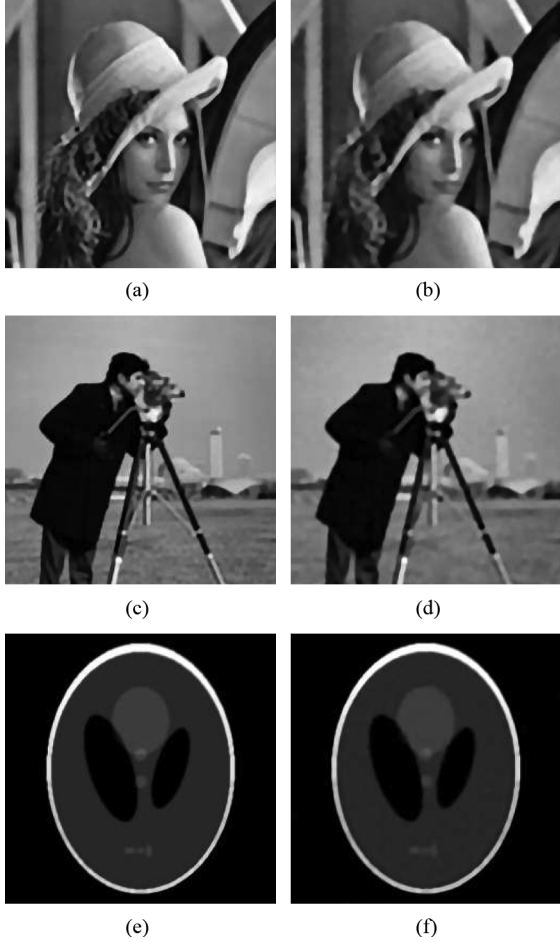


Fig. 9. Restored images. Gaussian PSF with variance 5, BSNR = 40 dB (left) and 20 dB (right).

3(c), and 3(d), and the restored images by nonblind deconvolution method [28] in Figs. 2, 3(e), and 3(f). In Table I, We see from the table that the performance of the proposed blind deconvolution algorithm is comparable to that of the nonblind deconvolution method. Visually the images restored by the proposed method method are quite competitive to those by the nonblind deconvolution method. We remark that an appropriate regularization parameter for the nonblind deconvolution method in [28] is manually selected. It is very time consuming to find the parameter to obtain such best results. However, in the proposed method, the two regularization parameters are estimated by the GCV method automatically. Finally, we show restoration SNR curves in Fig. 4. It can be observed that the approximations approach the true solution gradually.

#### B. Comparison With Blind Deconvolution Methods

We test the original images and PSFs which are displayed in Fig. 5. The observed images in Figs. 6–8 are obtained by blurring the original images with a Gaussian PSF with variances 9 and 5 respectively, and adding additive Gaussian noise BSNR = 40 dB and 20 dB, as these blurred and noisy images have been tested by TV1 and TV2 in [19]. The images restored by our proposed GCV-BD algorithm are shown in Figs. 7–9. In Tables II and III, we list the restoration results (ISNRs) by the

TABLE II  
COMPARISON IN ISNR ON GAUSSIAN PSF WITH VARIANCE 9

BSNR	Method	Lena	Cameraman	Shepp-Logan
40dB	GCV-BD	3.54	3.57	3.47
40dB	TV1 [19]	2.53	1.82	3.07
40dB	TV2 [19]	2.95	1.73	3.36
20dB	GCV-BD	2.60	3.56	3.75
20dB	TV1 [19]	2.62	1.70	2.47
20dB	TV2 [19]	-32.50	-40.89	-23.88

TABLE III  
COMPARISON IN ISNR ON GAUSSIAN PSF WITH VARIANCE 5

BSNR	Method	Lena	Cameraman	Shepp-Logan
40dB	GCV-BD	3.75	4.97	5.07
40dB	TV1 [19]	3.19	1.66	2.05
40dB	TV2 [19]	3.29	2.49	3.79
20dB	GCV-BD	3.32	4.63	4.84
20dB	TV1 [19]	1.39	1.43	2.09
20dB	TV2 [19]	-45.20	-42.54	-26.00

TABLE IV  
COMPARISON IN ISNR ON “CAMERAMAN” IMAGE

BSNR	PSF	GCV-BD	StStSt [8]	Method [18]
40dB	Guassian ( $\sigma^2 = 5$ )	4.97	2.82	1.32
40dB	Square (7 × 7)	8.40	8.31	4.06
20dB	Guassian ( $\sigma^2 = 5$ )	4.63	1.57	1.17
20dB	Square (7 × 7)	2.97	2.69	2.56

TV1, TV2 [19] and the proposed method. We see from the table that the performance of the proposed method is better than those of TV1 and TV2. In Fig. 10, we further show the 1-D slice of restored PSFs. We find that the PSF from TV1 and TV2 are about the same as the PSF estimated by the proposed method; see [19]. We remark that TV2 cannot give the PSF estimates when BSNR is 20 dB; see Table II.

Next we compare the proposed method with the recent variational Bayesian blind deconvolution algorithm (StStSt) [8], and the TV blind deconvolution algorithm [18]. Here we use “Cameraman” image with Gaussian PSFs to test the proposed method, same as the blurred and noisy images have been tested by StStSt and the TV blind deconvolution method in [8]. The results are shown in Table IV. We can observe that for the Gaussian PSF, the proposed method outperforms the other two methods. For the square PSF, both GCV-BD and StStSt have better results than the TV method when BSNR = 40 dB, but only have a little improvement when BSNR = 20 dB. To check the performance of the proposed algorithm on an image with texture, we use the “Lena” image as the testing image. We generate a blurred and noisy image using the 7 × 7 square PSF and Gaussian noise with variance  $\sigma^2 = 10^{-6}$ ; see [8]. We compare the images restored by three methods: StStSt, method in [18] and the proposed method. The ISNRs for these three methods are 5.29, 3.13, 6.19 respectively. These results may show that the proposed method can recover textured image quite well.

In [18], a “Satellite” image with a blur of disk [see Fig. 11(a)] is used to demonstrate the advantage of using the total variation function as the point spread function prior; see the model in (3). The blurred and noisy image is given in Fig. 11(b). Here, an additive Gaussian noise BSNR = 40 dB is added. We also employ the GCV method to estimate the regularization parameters for the terms of total variation of the image and the blur. We

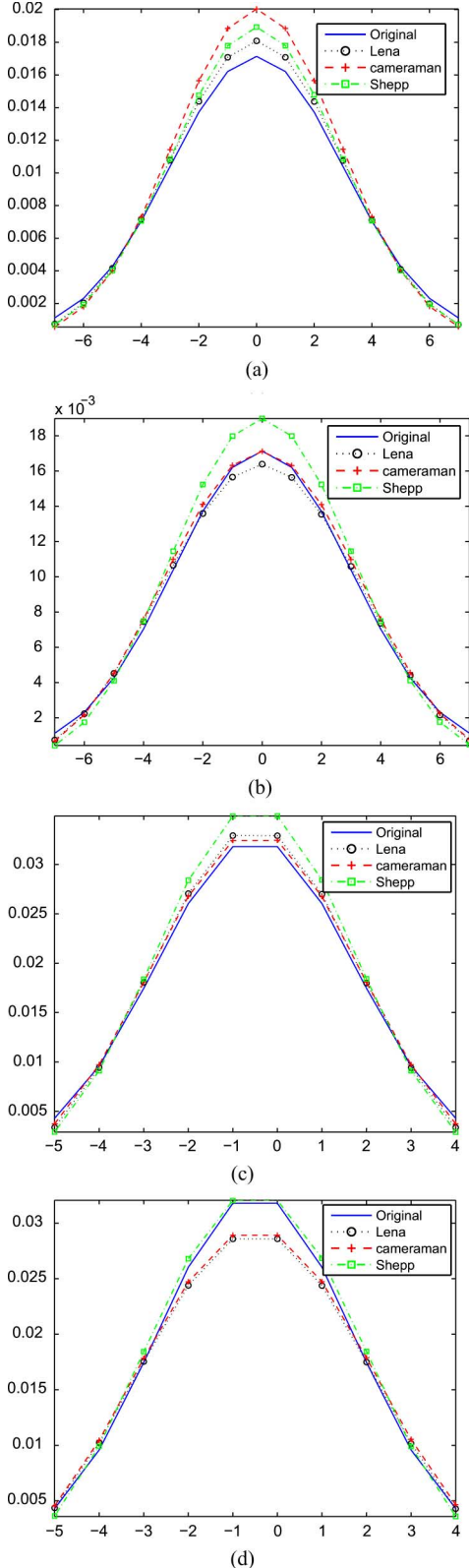


Fig. 10. 1-D slice of restored PSFs. (a) Guassian PSF with variance 9, BSNR = 40 dB. (b) Guassian PSF with variance 9, BSNR = 20 dB. (c) Guassian PSF with variance 5, BSNR = 40 dB. (d) Guassian PSF with variance 5, BSNR = 20 dB.

just use Algorithm 2 in Section II for estimating the image, the blur and their associated regularization parameters. For a comparison, we also tested 10 000 regularization parameter values

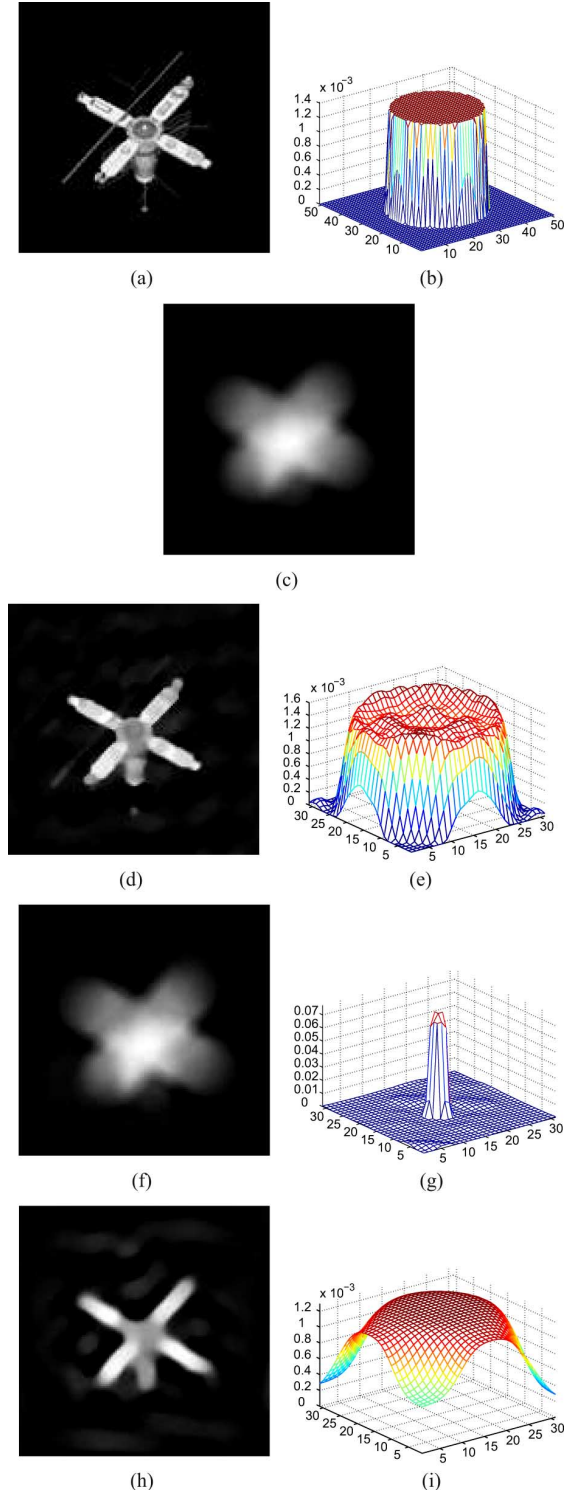


Fig. 11. Restoration results for the “Satellite” image. (a) Original image. (b) Blur. (c) Observed image. (d) Restored image [SNR = 11.57 dB] and (e) restored blur [SNR = 8.96 dB] by the proposed method. (f) Restored image [SNR = -1.44dB] and (g) restored blur [SNR = -19.56 dB] by using TV as the prior for the image and the blur and our parameter estimation method. (h) Restored image [SNR = 7.67 dB] and (i) restored blur [SNR = 3.94 dB] by using TV as the prior for the image and the blur for different tested parameters;  $\alpha_1$  and  $\alpha_2$  are  $5.86 \times 10^{-4}$  and 9.77.

and report the largest SNR of the resulting restored image. We remark that there is no hint in [18] how to select the regularization parameters in (3). In Fig. 11, we display the restored im-

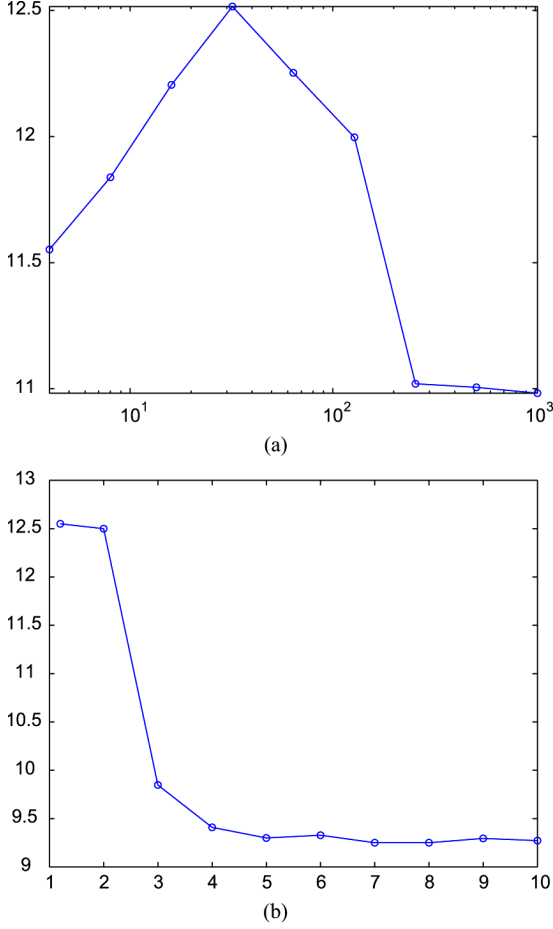


Fig. 12. Test on algorithm parameter setting. (a) Average SNRs with respect to different initial values of  $\beta$ . (b) Average SNRs with respect to different values of  $\theta$ .

ages and blurs. Although the proposed method cannot recover the edge of the blur exactly, we see that both the restored image and blur are visually better than those by the TV-blind algorithm. The SNRs of our restoration results are also better than those by the TV-blind algorithm. The GCV method for estimation of the two parameters in the TV-blind algorithm also fails; see Fig. 11(f) and (g).

### C. Sensitivity of Parameters

In Fig. 12, we show the sensitivity of two parameters  $\beta$  and  $\theta$  in Algorithm 2 for the SNRs of the restored images by the proposed blind deconvolution method. In Fig. 12(a), we fix the value of  $\theta$  (the multiplier) to be 1.2 and check the SNRs of the restored images for different initial values of  $\beta = 4, 8, 16, 32, 64, 128, 256, 512, 1024$ . Here, the “Lena” image is blurred by a Gaussian PSF with variance 9, then 40-dB noise is added to the blurred image; see Fig. 6(a). In Fig. 12(a), we display the average SNRs with respect to different initial values of  $\beta$ , and the average at each  $\beta$  is calculated based on ten runs of the algorithm. We see from the figure that the proposed blind deconvolution method can be sensitive to large initial value of  $\beta$ , and the SNRs of the restored images are lower when initial beta values are large. The reason is that the resulting image is about the same as  $g$  in Step 3 of Algorithm 2 as the

second term is dominant. Therefore, the restoration result may not be good. Therefore, we do not recommend to use a large initial value of  $\beta$  in the proposed image restoration process.

On the other hand, we fix the initial value  $\beta = 10$  and check SNRs of the restored images for different values of multiplier  $\theta = 1.2, 2, 3, 4, 5, 6, 7, 8, 9, 10$ . In Fig. 12(b), we display the average SNRs with respect to different values of  $\theta$ , and the average at each  $\theta$  is calculated based on 10 runs of the algorithm. We see from the figure that the proposed method can be sensitive to  $\theta$ . When  $\theta$  is greater than 2, the resulting SNRs of the restored images are significantly affected. For the proposed method, we find for  $1 < \theta \leq 2$  that the maximum difference among the SNRs of the restored images over their average SNRs is at most 1%. We remark in our previous tests in Sections III-A and III-B that  $\theta$  is set to 1.2.

### IV. CONCLUDING REMARKS

In this paper, we develop an algorithm for TV-based blind deconvolution. We regularize the image by the total variational norm and the blur by the squares of the Euclidean norm of the second order difference among the pixels, i.e., the total variation function is used as the image prior and a SAR model as the blur prior. Both the unknown image and blur can be estimated within alternating minimization framework. Using GCV method, the regularization parameters associated to the unknown image and blur can be updated in alternating minimization steps. Our experimental results have shown that the proposed algorithm is competitive with variational Bayesian blind deconvolution algorithms with Student’s-t priors or a total variation prior, in both improved SNRs and visual quality.

### REFERENCES

- [1] D. Kundur and D. Hatzinakos, “A novel blind deconvolution scheme for image restoration using recursive filtering,” *IEEE Trans. Signal Process.*, vol. 46, no. 2, pp. 375–390, Feb. 1998.
- [2] M. Ng, R. Plemmons, and S. Qiao, “Regularization of RIF blind image deconvolution,” *IEEE Trans. Image Process.*, vol. 9, no. 6, pp. 1130–1134, Jun. 2000.
- [3] C. Ong and J. Chambers, “An enhanced NAS-RIF algorithm for blind image deconvolution,” *IEEE Trans. Image Process.*, vol. 8, no. 7, pp. 982–992, Jul. 1999.
- [4] A. Katsaggelos and K. Lay, “Simltaneous blur identification and image restoration using the EM algorithm,” in *Proc. SPIE Conf. Visual Commun. Image Process. IV*, 1989, vol. 1199, pp. 1474–1485.
- [5] R. Lagendijk, A. Tekalp, and J. Bidmon, “Maximum likelihood image and blur identification: A unifying approach,” *Opt. Eng.*, vol. 29, pp. 422–435, 1990.
- [6] A. C. Likas and N. P. Galatsanos, “A variational approach for Bayesian blind image deconvolution,” *IEEE Trans. Signal Process.*, vol. 52, no. 8, pp. 2222–2233, Aug. 2004.
- [7] R. Molina, J. Mateos, and A. K. Katsaggelos, “Blind deconvolution using a variational approach to parameter, image, and blur estimation,” *IEEE Trans. Image Process.*, vol. 15, no. 12, pp. 3715–3727, Dec. 2006.
- [8] D. Tzikas, A. Likas, and N. Galatsanos, “Variational Bayesian sparse kernel-based blind image deconvolution with student’s-t priors,” *IEEE Trans. Image Process.*, vol. 18, no. 4, pp. 753–764, Apr. 2009.
- [9] S. Reeves and R. Mersereau, “Blur identification by the method of generalized crossvalidation,” *IEEE Trans. Image Process.*, vol. 1, no. 3, pp. 301–311, Jul. 1992.
- [10] J. W. Miskin and D. J. C. MacKay, “Ensemble learning for blind image separation and deconvolution,” in *Advances in Independent Component Analysis*, M. Girolami, Ed. New York: Springer-Verlag, 2000.
- [11] K. Z. Adami, “Variational methods in Bayesian deconvolution,” in *Proc. PHYSTAT 2003, SLAC*, Stanford, CA, 2003, pp. 8–11.
- [12] T. G. Stockham, T. M. Cannon, and R. B. Ingebretsen, “Blind deconvolution through digital signal processing,” *Proc. IEEE*, vol. 63, no. 4, pp. 678–692, Apr. 1975.

- [13] M. Cannon, "Blind deconvolution of spatially invariant image blurs with phase," *IEEE Trans. Acoust., Speech, Signal Process.*, vol. ASSP-24, no. 1, pp. 58–63, Jan. 1976.
- [14] R. G. Lane and R. H. T. Bates, "Automatic multidimensional deconvolution," *J. Opt. Soc. Amer. A*, vol. 4, no. 1, pp. 180–188, 1987.
- [15] R. Nakagaki and A. K. Katsaggelos, "A VQ-based blind image restoration algorithm," *IEEE Trans. Image Process.*, vol. 12, no. 9, pp. 1044–1053, Sep. 2003.
- [16] K. Panchapakesan, D. G. Sheppard, M. W. Marcellin, and B. R. Hunt, "Blur identification from vector quantizer encoder distortion," *IEEE Trans. Image Process.*, vol. 10, no. 3, pp. 465–470, Mar. 2001.
- [17] Y. You and M. Kaveh, "A regularization approach to joint blur identification and image restoration," *IEEE Trans. Image Process.*, vol. 5, no. 3, pp. 416–427, Mar. 1996.
- [18] T. F. Chan and C. K. Wong, "Total variation blind deconvolution," *IEEE Trans. Image Process.*, vol. 7, no. 3, pp. 370–375, Mar. 1998.
- [19] S. D. Babacan, R. Molina, and A. K. Katsaggelos, "Variational Bayesian blind deconvolution using a total variation prior," *IEEE Trans. Image Process.*, vol. 18, no. 1, pp. 12–26, Jan. 2009.
- [20] Y. You and M. Kaveh, "Blind image restoration by anisotropic regularization," *IEEE Trans. Image Process.*, vol. 8, no. 3, pp. 396–407, Aug. 1999.
- [21] Y. Huang and M. Ng, "Lipschitz and total-variational regularization for blind deconvolution," *Commun. Comput. Phys.*, vol. 4, pp. 195–206, Feb. 2008.
- [22] H. Liao, F. Li, and M. Ng, "Selection of regularization parameter in total variation image restoration," *J. Opt. Soc. Amer. A*, vol. 26, pp. 2310–2320, Nov. 2009.
- [23] Y. Yang, N. Galatsanos, and H. Stark, "Projection based blind deconvolution," *J. Opt. Soc. Amer. A*, vol. 11, no. 9, pp. 2401–2409, 1994.
- [24] D. Kundur and D. Hatzinakos, "Blind image deconvolution," *IEEE Signal Process. Mag.*, vol. 13, no. 3, pp. 43–64, Mar. 1996.
- [25] P. Campisi and K. Egiazarian, *Blind Image Deconvolution: Theory and Applications*. Boca Raton, FL: CRC, 2007.
- [26] L. Rudin, S. Osher, and E. Fatemi, "Nonlinear total variation based noise removal algorithms," *Physica D*, vol. 60, pp. 259–268, 1992.
- [27] T. Chan and K. Chen, "An optimization-based multilevel algorithm for total variation image denoising," *SIAM J. Multi. Model. Simul.*, vol. 5, pp. 615–645, 2006.
- [28] Y. Huang, M. Ng, and Y. Wen, "A fast total variation minimization method for image restoration," *SIAM J. Multiscale Model. Simul.*, vol. 7, pp. 774–795, 2008.
- [29] X. Guo, F. Li, and M. Ng, "A fast  $l_1$ -TV algorithm for image restoration," *SIAM J. Sci. Comput.*, vol. 31, pp. 2322–2341, 2009.
- [30] Y. Wang, J. Yang, W. Yin, and Y. Zhang, "A new alternating minimization algorithm for total variation image reconstruction," *SIAM J. Imaging Sci.*, vol. 1, pp. 248–272, 2008.
- [31] J. Yang, W. Yin, Y. Zhang, and Y. Wang, "A fast algorithm for edge-preserving variational multichannel image restoration," CAAM, Rice Univ., Houston, TX, Tech. Rep. 08-09.
- [32] M. Ng, *Iterative Methods for Toeplitz Systems*. Oxford, U.K.: Oxford Univ. Press, 2004.
- [33] A. Chambolle, "An algorithm for total variation minimization and applications," *J. Math. Imaging Vis.*, vol. 20, pp. 89–97, 2004.
- [34] M. Ng, L. Qi, Y. Yang, and Y. Huang, "On semismooth Newton's methods for total variation minimization," *J. Math. Imaging Vis.*, vol. 27, pp. 265–276, 2007.
- [35] G. Golub and U. V. Matt, "Generalized cross-validation for large scale problems," *J. Comput. Graph. Stat.*, vol. 6, pp. 1–34, 1997.
- [36] G. Golub, M. Heath, and G. Wahba, "Generalized cross-validation as a method for choosing a good ridge parameter," *Technometrics*, vol. 21, pp. 215–223, 1979.
- [37] M. Kilmer and D. O'leary, "Choosing regularization parameters in iterative methods for ill-posed problems," *SIAM J. Matrix Anal. & Appl.*, vol. 22, pp. 1204–1221, 2001.
- [38] G. Golub and G. Meurant, "Matrices, moments and quadrature," in *Numerical Analysis*, D. Griffiths and G. Watson, Eds. Essex, U.K.: Longman, 1994, pp. 105–156.
- [39] G. Forsythe, M. Malcolm, and C. Moler, *Computer Methods for Mathematical Computations*. Englewood Cliffs, NJ: Prentice-Hall, 1976.
- [40] R. Brent, *Algorithms for Minimization Without Derivatives*. Englewood Cliffs: Prentice-Hall, 1973.

**Haiyong Liao** received the B.Sc. and M.Phil. degrees from Shantou University, Shantou, China, in 2003 and 2006, respectively, and the Ph.D. degree from Hong Kong Baptist University, Kowloon Tong, Honk Kong.

After graduation, he was a Researcher with the Department of Mathematics, Hong Kong Baptist University, Kowloon Tong, Honk Kong. His main research interests are image restoration, inverse problems, and data mining.

**Michael K. Ng** received the B.Sc. and M.Phil. degrees from the University of Hong Kong, Hong Kong, in 1990 and 1992, respectively, and the Ph.D. degree from the Chinese University of Hong Kong, Hong Kong, in 1995.

He is a Professor with the Department of Mathematics at the Hong Kong Baptist University, Kowloon Tong. He was a Research Fellow with the Computer Sciences Laboratory, Australian National University (1995–1997), and an Assistant/Associate Professor (1997–2005) with the University of Hong Kong before joining Hong Kong Baptist University. He is the Programme Director of the M.Sc. Programme on Operational Research and Business Statistics and Director of the Centre for Mathematical Imaging and Vision (CMIV), Executive Director of the Institute for Computational Mathematics (ICM) at Hong Kong Baptist University. He has authored and edited five books and coauthored and authored more than 200 journal papers. He currently serves on the editorial boards of several international journals. As an applied mathematician, his main research areas include bioinformatics, data mining, operations research, and scientific computing.